Achieving Gaussian Multiple Access Channel Capacity With Spatially Coupled Sparse Graph Multi-User Modulation

Dmitri Truhachev*
*Department of Computing Science, University of Alberta, Edmonton, Canada, dmitryt@ualberta.ca

***Abstract*—Communication over a Gaussian multiple access channel (GMAC) is considered. Each user modulates his data as a superposition of redundant data streams. The interconnection of the modulated data symbols can be described by means of a sparse graph. The transmitted modulation graphs couple at the receiver, which performs joint detection based on iterative interference cancellation. We prove that the GMAC capacity can be achieved by such a system even for the case when all the users access the channel with equal power and transmit with equal rate.**

I. Introduction

The effect of spatial graph coupling, first discovered for convolutional low-density parity-check (LDPC) codes [1][2], have recently found applications in many areas of communications introducing a break-through in the area of iterative processing.

A protograph of a spatially coupled LDPC code is constructed by copying the protograph of an initial LDPC block code a number of times and connecting the neighboring copies by edges to form a graph chain. The graphs located at the ends of the chain contain variable nodes with fewer constraints, since these graphs are connected to their neighbors from only one side. As a result, iterative decoding progress initiates at the ends of the chain, due to the effect of the slight irregularity, and then propagates through the entire chain independently of the chain length. It has been shown [3], and then rigorously proved [4], that iterative decoding thresholds of spatially coupled LDPC codes coincide with the ML decoding thresholds of the closely related LDPC block codes that are, in turn, often close to the Shannon limit. This discovery attracted enormous interest to coupling phenomenon. The principle of spatial graph coupling has proven to be applicable to many areas, including multiple user detection [6], compressive sensing [7], and quantum coding [8].

In this paper, we apply spatial graph coupling to communication over the multiple access channel (MAC), representing a scenario in which a number of distinct transmitters send information to a single receiver. The corner points of the MAC capacity region polytope, which is known exactly, can be achieved by successive (onion peeling) decoding [10], while the middle part is achieved by rate splitting and/or time sharing added to the onion peeling [11]. On the other hand, multiuser communications techniques such as code-division multiple access (CDMA), that allow for more robust and less complex joint parallel detection/decoding have had limited success in achieving the inner points of the MAC capacity region. The case when all the users transmit with the same rate and power is typically the most difficult, since all the users happen to be operating under the same conditions, and there is no structural irregularity to initiate the decoding convergence. It has been shown that regular random CDMA can only support a fixed system load not exceeding $\alpha = 1.49$[1] [12] with equal power users, while sparse synchronous CDMA can support at most $\alpha = 2.07$ [13].

In this paper we consider a multiple access scheme in which each user modulates its data in form of multiple redundant data streams [13]. This format allows for sparse graph representation of the transmitted data. The transmitted signal graphs couple in the multiple access channel into a chain of graphs on which the receiver performs iterative interference cancellation and error correction decoding. In this work we demonstrate that the sparse graph modulation with spatial coupling can achieve multiple access AWGN channel capacity, and most importantly, the capacity can be achieved for the case of equal rate and power transmissions.

In particular, we show that for the case, when iterative decoding of component codes is performed at every interference cancellation iteration, the capacity can be achieved with low rate per-stream error correction codes and a large number of transmitted data streams. For the case in which multiple interference cancellation iterations are followed by a single error correction decoding round (two-stage detection/decoding schedule) the capacity is approached within a fraction of one bit/per dimension with use of error correction codes of rate close to 1, and with smaller number of data streams. Thus, depending on the balance between the number of interference cancellation and error correction iterations the near optimal communications can be achieved with a wide spectrum of rate vs. number of streams combinations.

[1]System load is defined as the ratio of supported number of users to the spreading gain (number of dimensions).

As a byproduct of the analysis we show that there is no limitation on the number of data streams which can be layered and decoded, i.e., any system load may be supported, (the property which was shown in [9] for the two-stage decoding). The latter property is also notable since linear interference cancellation methods such as zero-forcing or minimal-mean squared error (MMSE) usually cannot support loads much higher than $\alpha = 1$. Thus, sparse graph modulation with iterative parallel interference cancellation reception establishes literally a universal multiple access technique.

II. System Model

We consider a multiuser modulation format based on generalized modulation [14]. The kth user $k \in \{1, 2, \ldots, K\}$ transmits a vector of binary data $\{u_{k,l}\}_{l=1}^{L}$, encoded by a binary error correction code. The data is multiplexed into M identical data streams $\{u_{k,m,l}\}_{l=1}^{L}$ which are modulated in parallel. During the modulation phase each data stream $\{u_{k,m,l}\}_{l=1}^{L}$ is permuted by an interleaver $\pi_{k,m}$ to produce a permuted stream $\{\tilde{u}_{k,m,l}\}_{l=1}^{L}$. Each bit of the permuted stream $\{\tilde{u}_{k,m,l}\}_{l=1}^{L}$ is multiplied by an N-dimensional signature sequence $\boldsymbol{s}_{k,m}$. The N dimensions represent the resource space and can, for example, be time or frequency slots. This operation is similar to spreading operation in CDMA systems. The M modulated streams are summed up and multiplied by the amplitude $\sqrt{\frac{P_k}{M}}$ to produce the modulated signal of user k

$$\boldsymbol{v}_{k,l} = \sum_{m=1}^{M} \sqrt{\frac{P_k}{M}} \tilde{u}_{k,m,l} \boldsymbol{s}_{k,m} \quad l = 1, 2, \ldots, L \ . \tag{1}$$

We consider the case in which every signature sequence $\boldsymbol{s}_{k,m} = \{s_{k,m,1}, s_{k,m,2}, \ldots, s_{k,m,N}\}$ is real and energy normalized such that $\mathbb{E}|s_{k,m,i}|^2 = \frac{1}{N}$, $i = 1, 2, \ldots, N$. We also require the average energy of the correlation between any distinct sequences to be equal to $1/N$ [2] i.e., $\mathbb{E}\boldsymbol{s}_{k_1,m_1}\boldsymbol{s}_{k_2,m_2}^{\mathrm{T}} = 1/N$, $(k_1, m_1) \neq (k_2, m_2)$. In this paper we focus on transmission over a real-valued Gaussian multiple access channel with noise power σ^2. The powers of the users' signals are $P_k = 1$, $k = 1, 2, \ldots, K$.

Note that the interconnection of the data bits in each user's signal can be represented by means of a graph. The bipartite graph representing one signal connects L variable nodes corresponding to the data bits $u_{k,l}$, $l = 1, 2, \ldots, L$ and the L channel nodes, representing the addition of the M data signals $\tilde{u}_{k,m,l}\boldsymbol{s}_{k,m}$, $m = 1, 2, \ldots, M$. In the considered sparse graph representation each data bit $u_{k,l}$ is connected to M channel nodes corresponding to the times at which the M replicas of $u_{k,l}$ are transmitted over the channel. For the case when $L \gg K, M$ the modulation graphs of the users are sparse.

[2]The following property can be easily guaranteed by choosing $s_{k,m,i} \in \left\{-\frac{1}{\sqrt{N}}, \frac{1}{\sqrt{N}}\right\}$ iid Bernoulli with probability $1/2$. However, other signature sequence choices are also possible.

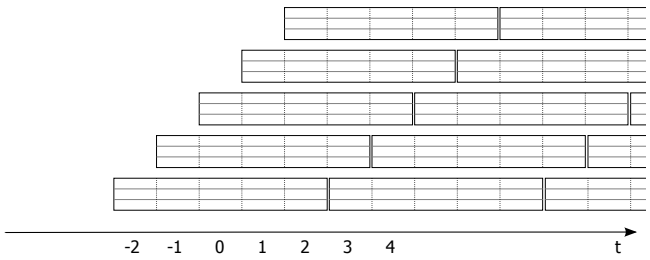

Fig. 2. Transmitted packets coupling in the channel, $W = 2$.

Once the users transmit their data with the time offsets[3] their transmitted signal graphs couple in the channel. This process is illustrated in Fig 1. The variable nodes of the signal modulation graphs are illustrated by magenta circles, while the multiple access nodes are given by green hexagons. Fig 1 a) illustrates individual signal graphs and Fig 1 b) illustrates the graph coupling. The consecutive graphs become connected in the channel and form a chain.

We consider a situation in which the number of users equals $K = 2W + 1$. The packets, transmitted by the users and represented by the modulation graphs, overlap as shown in Fig. 2. We assume that each packet consists of $2W+1$ sections of length $L/(2W + 1)$ bits each. The $M \gg W$ replicas of each data bit $u_{k,l}$ are distributed uniformly among the $2W+1$ sections of the packet. Each packet consists of one data stream modulated by a user. The M data sub-streams of each packet are illustrated by bars within a box depicting a packet. We assume that the fist user starts to transmit his packets at time $t = -W$ (if time is given in terms of sections). Then, at $t = -W + 1$ the second user joins the transmission. At time $t = -W + 2$ the third user joins and so on. As a result, the first section of the first transmitted packet does not face interference with any other packets. The second section of the first packet of the 1st user interferes with the first section of the first packet of 2nd user, and so on.

The receiver observes a composite signal, consisting of the transmitted users' data streams and the additive noise, and performs iterative decoding. We consider two types of receivers. The first receiver, which we call the *two stage* receiver, performs iterative interference cancellation layering the user's signal which is followed by individual error correction decoding which is performed for all the users in parallel. Thus, the first, iterative interference cancellation stage, is separated from the second, error correction decoding stage. The second receiver, which we call a *modified successive interference cancellation (SIC)* receiver performs error correction decoding at every interference cancellation iteration. We assume, however, that the decoding is performed only for the users those signal-to-noise and interference ratio (SINR) is greater

[3]Offsets happen in the resource space in general. The resource space needs not necessarily be the time.

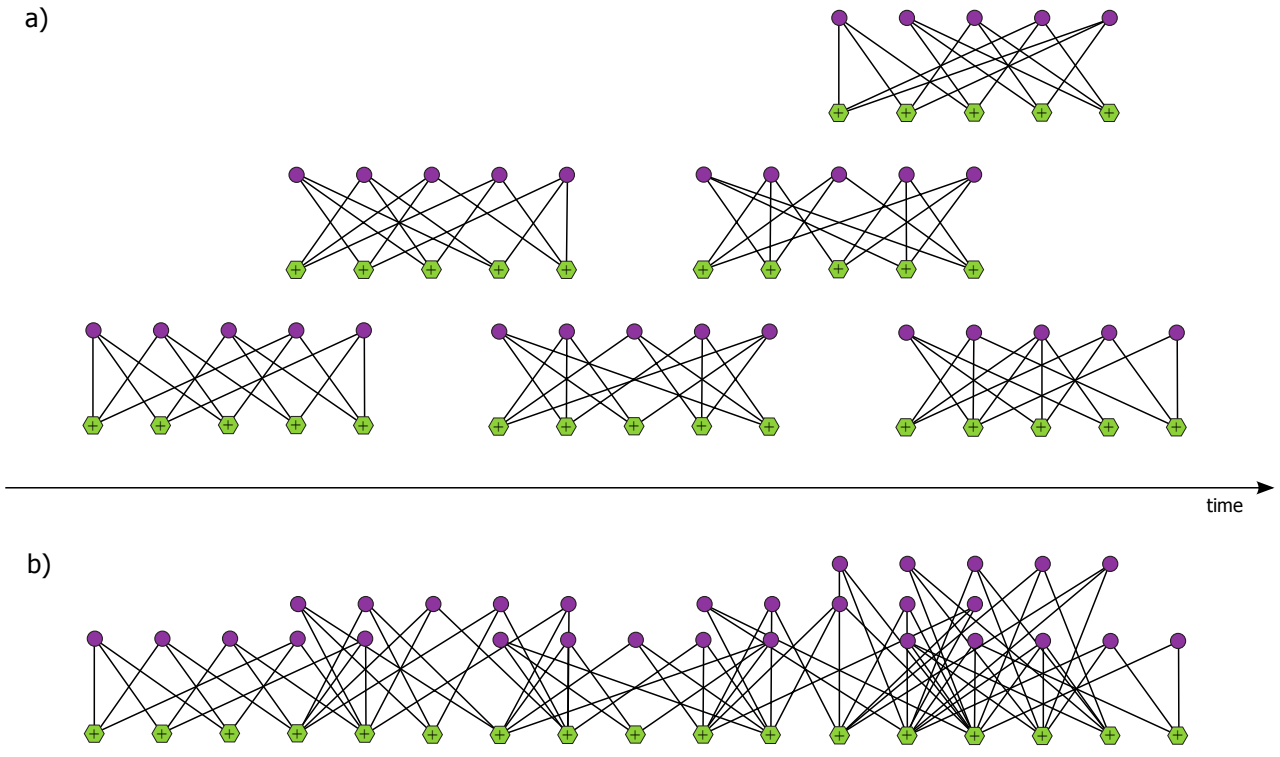

Fig. 1. Distinct sparse modulation graphs (Fig. a)) coupling on-the-fly (Fig. b)).

that the threshold θ of the error correction code used for data encoding. Thus, at every iteration the users with SINR greater than θ are decoded and removed from the system, while the remaining users are not decoded and only participate in the interference cancellation process. As the interference cancellation progresses with the iterations, more and more users' signals become decoded and removed from the system, thus, decreasing the interference pool.

The, iterative interference cancellation is performed as follows. Assume that the M replicas $u_{k,m,l}$, $m = 1, 2, \ldots, M$ of the data bit $u_{k,l}$ are transmitted over the channel at times $t_1, t_2, \ldots, t_M$. At the first iteration we perform matched filtering of the received signal using $\boldsymbol{s}_{k,m}$, $k = 1, 2, \ldots, K$, $m = 1, 2, \ldots, M$. The filtered signal at the time t_m is

$$\begin{aligned} q_{k,m,t_m} &= \frac{1}{\sqrt{M}} \boldsymbol{s}_{k,m}^{\mathrm{T}} \big(u_{k,m,l} \boldsymbol{s}_{k,m} + \sum_{(k_1,m_1)\neq(k,m)} \tilde{u}_{k_1,m_1,t_m} \boldsymbol{s}_{k_1,m_1} \big) \\ &= \frac{1}{\sqrt{M}} u_{k,m,l} + I_{k,m,t_m} \end{aligned} \tag{2}$$

Thus, the filtered signal consists of the signal term $\frac{1}{\sqrt{M}} u_{k,m,l}$ of power $1/M$ and the interference term I_{k,m,t_m} of power x_{k,m,t_m}. The power of the interference term depends on the time t_m and the position of the $u_{k,m,l}$ within its packet. The interference power decreases with interference cancellation iterations.

We use the M filtered signals q_{k,m,t_m} to create M different estimates of the data bit $u_{k,l}$. Each estimate is based on $M-1$ signals; one signal is excluded. The estimates are formed as

$$\hat{u}_{k,m,l} = \tanh \left(\sum_{m' \neq m} \xi_{k,m',t_{m'}} q_{k,m',t_{m'}} \right) , \tag{3}$$

where the weighting coefficients $\xi_{k,m',t_{m'}}$ are computed based of the interference power

$$\xi_{k,m',t_{m'}} = \frac{1}{x_{k,m,t_m}} \left(\sum_{m'=1}^{M} \frac{1}{x_{k,m',t_{m'}}} \right)^{-1}$$

The SINR of the expression inside the parenthesis in (3) equals

$$z_{k,m,l} = \frac{1}{M} \sum_{m' \neq m} \frac{1}{x_{k,m',t_{m'}}} . \tag{4}$$

The bit estimates $\hat{u}_{k,m,l}$ are utilized to reconstruct the transmitted signals. The reconstructed signals $\hat{\boldsymbol{v}}_{k,l}$ are used to perform interference cancellation. During the interference cancellation phase the $K-1$ reconstructed signals, all except the kth signal are subtracted from the received signal

$$\tilde{\boldsymbol{v}}_{k,l}^{(1)} = \boldsymbol{r}_l - \sum_{k' \neq k} \hat{\boldsymbol{v}}_{k,l}$$

to produce signals $\tilde{\boldsymbol{v}}_{k,l}^{(1)}$ with partially cancelled interference and noise. At the second iteration, the signals $\tilde{\boldsymbol{v}}_{k,l}^{(1)}$ are filtered again, the filtered signals are used to estimate the data bits and so on. The two-stage decoder repeats this operation, which is the first stage, I times (I iterations) and then passes the signals to the error control decoding (second stage). The modified SIC decoder does the error correction after every interference cancellation iteration, but only for the signals, which have the SINR greater than the threshold θ. The sparsity of the modulation graph decreases the chances of short loops to appear in the graph. The absence of short loops, in turn, ensures that the information derived from various received replicas of the data bits is not used multiple times during the iterative processing. This is a common restriction in the iterative decoding frameworks.

III. Analysis

We start with the analysis of the two-stage receiver. The first, iterative interference cancellation stage, can be analyzed as follows. Let us denote the composite noise-and-interference variance experienced by each user's data bits transmitted at time t by x_0^t. The noise-and-interference variance is reduced from x_0^t to $x_i^t < x_0^t$ after i interference cancellation iterations. The SINR of the data bits of the packet, that starts at time $t-W$ and finishes at $t+W$, considered at iteration i, is denoted by z_i^t. Thus, the upper index t of the above mentioned variables, characterizing system's dynamics, indicates the time slot of interest, and i is the iteration number. By y_i^t we denote the average mean squared error of the data bits of the packet which starts at time $t-W$ and finishes at $t+W$ (packet centered at time t) at iteration i. A discrete system of equations describing the evolution of x_i^t, y_i^t, and z_i^t have been derived in [5] and is given by

$$x_i^t = \frac{\alpha}{2W+1}\sum_{j=-W}^{W} y_i^{t+j} + \sigma^2 \qquad i \geq 0, t \geq 1 \tag{5}$$

$$z_i^t = \frac{1}{2W+1}\sum_{j=-W}^{W} \frac{1}{x_{i-1}^{t+j}} \qquad i > 0, t \geq W+1 \tag{6}$$

$$y_i^t = g\left(z_i^t\right) \qquad i > 0, t \geq W+1 \tag{7}$$

where the function $g(\cdot)$ is given by

$$g(a) = \mathbb{E}\left[\left(1-\tanh\left(a+\xi\sqrt{a}\right)\right)^2\right] \ , \quad \xi \sim \mathcal{N}(0,1) \ ,$$

where $\mathcal{N}(0,1)$ denotes a standard normal random variable.

Equation (5) is determined from the fact that only the packets that start between time $t-2W$ and t contribute to the noise-and-interference variance at time t. SINR z_i^t is computed from the SINRs of the M partitions uniformly distributed along the packet. The SINRs $\frac{1}{x_{i-1}^{t+l}}$ of the partitions are averaged in (6), just like in (4). Function $g(\cdot)$, introduced in [17], is strictly decreasing from $g(0)=1$ to $g(+\infty)=0$.

The initialization of the iterative system is as follows. The transmission starts at time $-W$. Therefore, we assume that all the packets centered at time $t < -W$ are perfectly known (since they do not exist) and

$$z_0^t = +\infty \qquad t < -W \tag{8}$$

$$y_0^t = 0 \qquad t < -W \ . \tag{9}$$

On the other hand, the packets which start to arrive are completely unknown and, therefore,

$$z_0^t = 0 \qquad t \geq -W \tag{10}$$

$$y_0^t = 1 \qquad t \geq -W \ , \tag{11}$$

and

$$x_0^t = 0 \quad t \leq -W \ , \tag{12}$$

$$x_0^t = \frac{\alpha t}{2W+1} + \sigma^2; \quad t \in [-W, W] \tag{13}$$

$$x_0^t = \alpha + \sigma^2 \quad t > W \tag{14}$$

A. Continuous System Dynamics Model

To construct a variance and SINR evolution model that is continuous in time, we normalize packet length to 1 and let the number of segments $W \to \infty$. Then the equations (5)–(7) can be transformed into

$$x_i^t = \alpha \int_{-1/2}^{1/2} y_i^{t+\tau} d\tau + \sigma^2 \qquad t \geq -\frac{1}{2}, i \geq 0 \tag{15}$$

$$z_i^t = \int_{-1/2}^{1/2} \frac{1}{x_{i-1}^{t+\tau}} d\tau \qquad t \geq 0, i > 0 \tag{16}$$

$$y_i^t = g\left(z_i^t\right) \qquad t \geq 0, i > 0 \tag{17}$$

The above equations also accommodate a shift by $1/2$ to the right along the time axis. This shift, indicating that the transmission starts at time 0, is performed for notation simplicity. The dynamic system (15)–(17) is initialized using a function

$$z_0^t = \begin{cases} +\infty, & t < 0 \\ 0, & t \geq 0 \ , \end{cases} \tag{18}$$

or equivalently

$$y_0^t = \begin{cases} 0, & t < 0 \\ 1, & t \geq 0 \ . \end{cases} \tag{19}$$

The equations (15)–(17) describe the first, interference cancellation stage of the two-stage receiver. Thus, the SINR of the data bits of the packet centered at time t, at iteration I of the interference cancellation stage equals z_I^t. The second, error correction decoding stage, is successful if $z_I^t > \theta$ where θ is the error correction code threshold.[4]

[4]We assume that strong error correction codes, that exhibit threshold behavior, are used for data encoding. For SINRs above the threshold a communication, that is essentially error free, is possible, while for SINRs below the threshold error correction capability of the codes is very limited. This type of behavior is typical for LDPC and turbo codes.

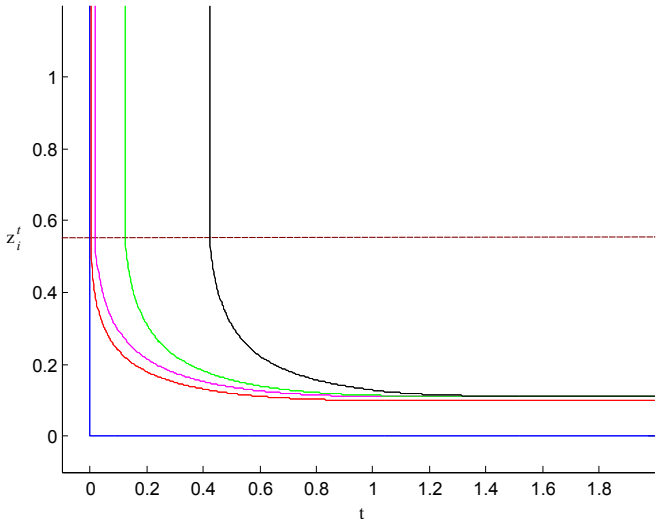

Fig. 3. SINR functions $z^t_{\mathrm{SIC},i}$ for iteration numbers $i = 0, 1, 2, 10, 30$ (curves from left to right), $\alpha = 10$, $\sigma^2 = 0.01$ and $\theta = 0.55$.

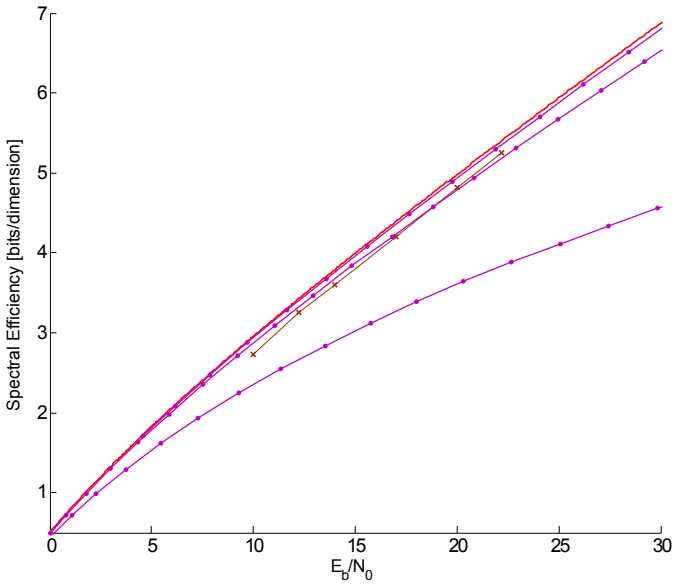

Fig. 4. Achievable spectral efficiency for the modified SIC receiver (magenta), two-stage receiver (brown) and the AWGN channel capacity (red).

While the two-stage receiver starts with I interference cancellation iterations and then performs error correction decoding once, the modified SIC receiver is performing error correction decoding after every interference cancellation iteration. Again we can determine the success of the decoding by comparing the current SINR of the packet $z^t_{\mathrm{SIC},i}$ to the iterative decoding threshold θ. Therefore, the dynamics of the modified SIC can be described by

$$x^t_{\mathrm{SIC},i} = \alpha \int_{-1/2}^{1/2} y^{t+\tau}_{\mathrm{SIC},i} d\tau + \sigma^2 \qquad t \geq -\frac{1}{2}, i \geq 0 \qquad (20)$$

$$y^t_{\mathrm{SIC},i} = g\left(z^t_{\mathrm{SIC},i}\right) \qquad t \geq 0, i > 0 \qquad (21)$$

together with

$$z^t_{\mathrm{SIC},i} = \begin{cases} +\infty, & \int_{-1/2}^{1/2} \frac{1}{x^{t+\tau}_{\mathrm{SIC},i-1}} d\tau > \theta \\ \int_{-1/2}^{1/2} \frac{1}{x^{t+\tau}_{\mathrm{SIC},i-1}} d\tau, & \int_{-1/2}^{1/2} \frac{1}{x^{t+\tau}_{\mathrm{SIC},i-1}} d\tau \leq \theta \end{cases} . \qquad (22)$$

IV. Results

Let us start with a numerical illustration of the convergence process of the modified SIC receiver. Consider a system load $\alpha = 10$ and the noise power $\sigma^2 = 0.01$. The error control coding threshold is set to $\theta = 0.55$. The functions $z^t_{\mathrm{SIC},i}$ corresponding to the SINRs of packets centered at time t computed at iteration i are shown in Fig. 3. The blue curve corresponds to the initial SINR $z^t_{\mathrm{SIC},0}$, the red curve corresponds to $z^t_{\mathrm{SIC},1}$, the magenta curve to $z^t_{\mathrm{SIC},2}$, the green curve to $z^t_{\mathrm{SIC},10}$, and finally, the black curve corresponds to $z^t_{\mathrm{SIC},30}$. The level of the threshold θ is given by the horizontal brown line.

Note, that $z^t_{\mathrm{SIC},i} = \infty$ for $t < T_i$ as illustrated by the figure. The time T_i represent the cutoff time at iteration i. All packets transmitted before T_i are already decoded by iteration i, while the packets transmitted after T_i are still in the decoding process. The curves demonstrate that T_i is increasing with a constant speed as a function of the iteration number i. The speed of the decoding convergence is given by $s = \lim_{i\to\infty}(T_i - T_{i-1})$. For a given load α and noise power σ^2 the speed s is a function of the error correction decoding threshold θ, i.e., $s = s(\theta)$. Moreover, it can be observed that $s(\theta)$ is a decreasing function of θ.

For some limiting value of $\theta = \theta_{\max}$ the convergence stops and the speed $s(\theta_{\max}) = 0$. This limiting value $\theta_{\max}(\alpha, \sigma^2)$ exists for any combination of α and σ^2 since the achievable SINR is always smaller than $1/\sigma^2$, indicating the so called "single user performance". We recall that the power of each user's signal equals to 1.

Consider now communication employing error correction codes which are capacity achieving on the binary input AWGN channel (BIAWGN) with SINR θ. In this case the spectral efficiency of the entire system (in bits per dimension) equals

$$\mathcal{C}_{\mathrm{eff}} = \alpha C_{\mathrm{BIAWGN}}(\theta) \qquad (23)$$

which is, of course, only achievable if the system converges for this value of θ. Therefore, for any given α and σ^2 the maximum achievable spectral efficiency equals

$$\mathcal{C}_{\mathrm{eff}}(\alpha, \sigma^2) = \alpha C_{\mathrm{BIAWGN}}(\theta_{\max}(\alpha, \sigma^2)) . \qquad (24)$$

since $\theta_{\max}(\alpha, \sigma^2)$ is the largest value of θ, for which the system still converges.

The next two theorems demonstrate that the spectral efficiency $\mathcal{C}_{\mathrm{eff}}(\alpha, \sigma^2)$ (24) is in fact converging to the channel

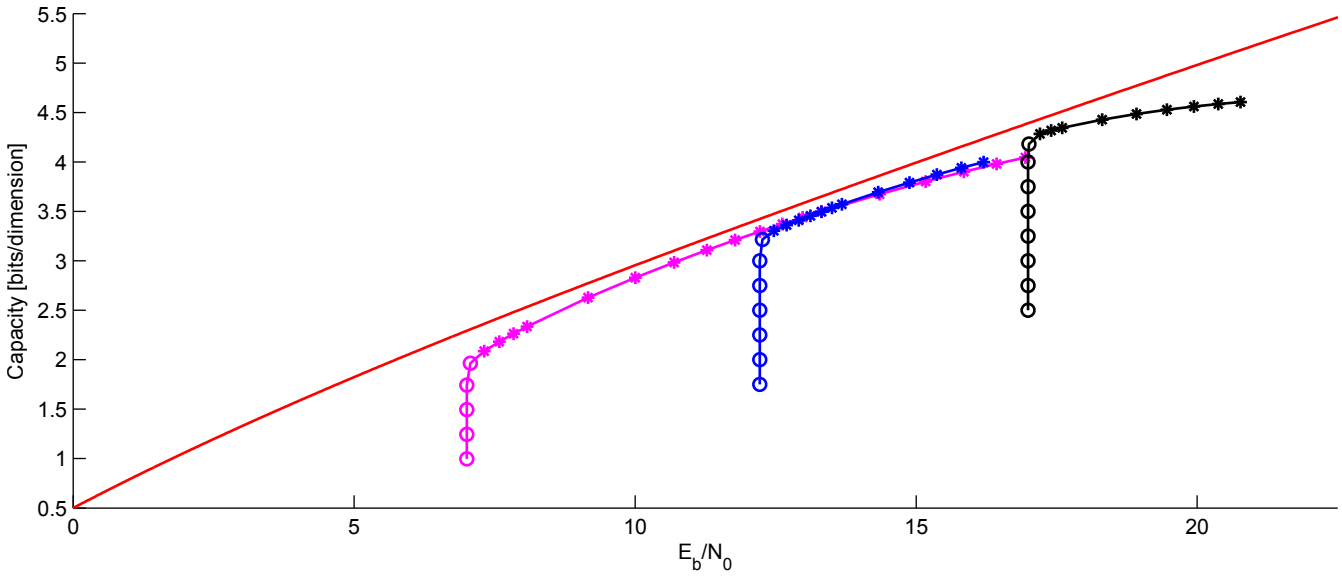

Fig. 5. Achievable spectral efficiencies for $\sigma^2 = 0.1$ and $\alpha \in [1, 30]$ (magenta), $\sigma^2 = 0.03$ and $\alpha \in [1.75, 10]$ (blue), and $\sigma^2 = 0.01$ and $\alpha \in [2.5, 10]$ (black). The AWGN channel capacity is shown by the red curve. The SNR E_b/N_0 is given in dB.

capacity itself, i.e., the GMAC capacity can be achieved by the modified SIC receiver.

Theorem 1. *[15] Spectral efficiency of*

$$\alpha \mathcal{C}_{\mathrm{BIAWGN}}\left(\frac{1}{\alpha}\ln\frac{\alpha+\sigma^2}{\sigma^2} - \epsilon\right) \tag{25}$$

is achievable by the modified SIC receiver for any $\alpha \in [0, \infty)$ and $\epsilon > 0$. The achieved speed of convergence approximately equals $s = \epsilon\sigma^2(\alpha + \sigma^2)/\alpha$.

Let us define the total system SNR parameter $\xi = \frac{\alpha}{\sigma^2}$. The next theorem states that for any fixed ξ the AWGN channel capacity is achievable by the modified SIC decoder. Let us consider $\sigma^2 = \alpha/\xi$, i.e., we are keeping ξ fixed. We denote the limiting spectral efficiency of the system considered in Theorem 1 and the corresponding SNR per bit by

$$\mathcal{C}_{\mathrm{eff}}(\alpha, \xi) = \alpha \mathcal{C}_{\mathrm{BIAWGN}}\left(\frac{1}{\alpha}\ln(1+\xi)\right) \tag{26}$$

$$\frac{E_\mathrm{b}}{N_0}(\alpha, \xi) = \frac{1}{2\mathcal{C}_{\mathrm{BIAWGN}}\left(\frac{1}{\alpha}\ln(1+\xi)\right)\sigma^2}\,. \tag{27}$$

We also define the real-valued AWGN channel capacity $\mathcal{C}_{\mathrm{AWGN}}\left(\frac{E_\mathrm{b}}{N_0}\right)$ for given $\frac{E_\mathrm{b}}{N_0}$ as the root of the equation

$$\mathcal{C}_{\mathrm{AWGN}}\left(\frac{E_\mathrm{b}}{N_0}\right) = \frac{1}{2}\log_2\left(1 + 2\mathcal{C}_{\mathrm{AWGN}}\left(\frac{E_\mathrm{b}}{N_0}\right)\frac{E_\mathrm{b}}{N_0}\right)\,. \tag{28}$$

Theorem 2. *[15]*

$$\lim_{\alpha\to\infty} \mathcal{C}_{\mathrm{eff}}(\alpha, \xi) = \lim_{\alpha\to\infty} \mathcal{C}_{\mathrm{AWGN}}\left(\frac{E_\mathrm{b}}{N_0}(\alpha, \xi)\right) = \frac{1}{2}\log_2(1+\xi)$$

Spectral efficiency $\mathcal{C}_{\mathrm{eff}}(\alpha, \xi)$ achieved by the modified SIC receiver (see Theorem 1) is plotted in Fig. 4. The three magenta curves correspond to $\alpha = 10, 100$, and 500 (from bottom to top). For each curve α is kept constant while ξ is varying. The channel capacity $\mathcal{C}_{\mathrm{AWGN}}$ is given by the blue curve. Finally, the brown curve plots spectral efficiency achieved by the two-stage receiver.

Finally we present a more detailed computation results on the maximum achievable spectral efficiency. Fixing the noise power σ^2 we plot the achievable C_{eff} as a function of the load α. For each α, the $\theta_{\mathrm{max}}(\alpha, \sigma^2)$ is computed and then used to calculate $C_{\mathrm{eff}}(\alpha, \sigma^2)$ using (24). The magenta curve in Fig. 5 corresponds to $\sigma^2 = 0.1$ and $\alpha \in [1, 30]$, the blue curve corresponds to $\sigma^2 = 0.03$ and $\alpha \in [1.75, 10]$, and the black curve corresponds to $\sigma^2 = 0.01$ and $\alpha \in [2.5, 10]$. All the curved are plotted as functions of E_b/N_0 and are compared to the GMAC capacity (red curve).

Each of the σ^2 curves starts at lower E_b/N_0 and continues towards higher E_b/N_0 as α increases. The points, shown by circles, are achievable by both the two-stage decoding and the modified SIC decoding, while the points given by stars are only achievable by the modified SIC. Note, the some circle points are always located at the part of each curve which is the closest to the channel capacity. Based on this observation we conclude, the the low-complexity two-stage decoding is sufficient for approaching the GMAC capacity closely.

V. Conclusions

In this paper, it has been shown that sparse graph modulation with spatial coupling can achieve AWGN channel capacity under modified SIC reception and closely approach it with the two-stage reception method, in which iterative interference cancellation is separated from the error correction decoding.

REFERENCES

[1] A. Jiménez Felström and K. Sh. Zigangirov, "Time-varying periodic convolutional codes with low-density parity-check matrices," *IEEE Transactions on Information Theory*, vol. IT-45, no. 6, pp. 2181–2191, September 1999.

[2] D. Truhachev, M. Lentmaier, and K. S. Zigangirov, "Mathematical analysis of iterative decoding of ldpc convolutional codes," in *Proccedings of the 2001 IEEE International Symposium on Information Theory*, Washington, USA, June 2001.

[3] M. Lentmaier, A. Sridharan, D. J. Costello, Jr., and K. Sh. Zigangirov, "Iterative decoding threshold analysis for LDPC convolutional codes," *IEEE Trans. Inf. Theory*, vol. 56, no. 10, pp. 5274–5289, Oct. 2010.

[4] S. Kudekar, T. Richardson, and R. Urbanke, "Threshold saturation via spatial coupling: why convolutional LDPC ensembles perform so well over the BEC," in *Proc. IEEE Int. Symp. on Inf. Theory*, Austin, TX, June 2010.

[5] C. Schlegel and D. Truhachev, "Multiple Access Demodulation in the Lifted Signal Graph with Spatial Coupling," in *Proc. IEEE Int. Symp. on Inf. Theory*, St. Petersburg, Russia, Aug. 2011.

[6] K. Takeuchi, T. Tanaka, and T. Kawabata, "Improvement of BP-based CDMA multiuser detection by spatial coupling," in *Proc. IEEE Int. Symp. on Inf. Theory*, St. Petersburg, Russia, Aug. 2011.

[7] S. Kudekar and H. D. Pfister, "The effect of spatial coupling on compressive sensing," in *Proc. Allerton Conf. on Communications, Control, and Computing*, Monticello, IL, Sept. 2010.

[8] M. Hagiwara, K. Kasai, H. Imai, and K. Sakaniwa, "Spatially coupled quasi-cyclic quantum LDPC codes," in *Proc. IEEE Int. Symp. on Inf. Theory*, St. Petersburg, Russia, Aug. 2011.

[9] C. Schlegel and D. Truhachev,"Multiple Access Demodulation in the Lifted Signal Graph with Spatial Coupling," *IEEE Transactions on Information Theory*, under revision, March 2011.

[10] T. Cover and J. Thomas, *Elements of Information Theory*, Wiley & Sons, New York, 2006.

[11] B. Rimoldi and R. Urbanke, "A Rate Splitting Approach to the Gaussian Multiple Acess Channel" *IEEE Trans. on Inf. Theory*, vol. 42, no. 2, pp. 364–375, Mar. 1996.

[12] T. Tanaka "A statistical mechanics approach to large-system analysis of CDMA multiuser detectors", *IEEE Trans. Inf. Theory*, vol. 48, no. 11, pp. 2888–2910, Nov. 2002.

[13] D. Truhachev, C. Schlegel and L. Krzymien, "A Two-Stage Capacity Achieving Demodulation/Decoding Method for Random Matrix Channels", *IEEE Trans. on Inf. Theory*, vol. 55, pp. 136–146, Jan. 2009.

[14] C. Schlegel, M. Burnashev, and D. Truhachev, "Generalized Superposition Modulation and Iterative Demodulation: A Capacity Investigation," *Hindawi Journal of Electrical and Computer Engineering*, vol. 2010, Sep. 2010.

[15] D. Truhachev, "Achieving AWGN Multiple Access Channel Capacity with Spatial Graph Coupling," *IEEE Communications Letters*, under revision, Jan. 2012. [Online]. Available: http://arxiv.org/abs/1111.3696

[16] R. Gallager, *Information Theory and Reliable Communications*, Wiley & Sons, New York, 1968.

[17] M. Burnashev, C. Schlegel, W. Krzymien, and Z. Shi, "Characteristics Analysis of Successive Interference Cancellation Methods", *Problemy Peredachi Informatsii*, vol. 40, no. 4, pp. 297–317, Dec. 2004.